Properties of isospin asymmetric quark matter in quark stars

Peng-Cheng Chu,[1,*] Xiao-Hua Li,[2,3,†] He Liu,[1,‡] Min Ju,[4,§] and Ying Zhou[5,‖]

[1]*The Research Center for Theoretical Physics, Science School, Qingdao University of Technology, Qingdao 266033, China*

[2]*School of Nuclear Science and Technology, University of South China, Hengyang 421001, China*

[3]*Cooperative Innovation Center for Nuclear Fuel Cycle Technology & Equipment, University of South China, Hengyang 421001, China*

[4]*College of Science, China University of Petroleum (East China), Qingdao 266580, China*

[5]*School of Physical Science and Technology, Inner Mongolia University, Hohhot 010021, China*

(Received 9 April 2023; accepted 2 August 2023; published 16 August 2023)

In this work, we explore the properties of isospin asymmetric quark matter in quark stars (QSs). The isospin chemical potential, the isospin asymmetry, the quark matter symmetry energy, the equation of state (EOS) of strange quark matter (SQM), and the maximum mass of QSs are also studied by using different quark phenomenological models. Our results indicate that the parameter space of the quark phenomenological models for the quark matter symmetry energy and the EOS of the star matter can be reduced by considering the recent mass-radius estimates of PSR J0740 + 6620, PSR J0030 + 0451, 4U 1702-429, and the central compact star within the supernova remnant HESS J1731-347.

DOI: 10.1103/PhysRevC.108.025808

I. INTRODUCTION

Investigating the properties of the equation of state (EOS) of strongly interacting matter is one of the major science goals of terrestrial nuclear laboratory experiments and astrophysical laboratory observations, which is of significance in understanding the nuclear reactions and the matter state of the early universe [1–4]. The compact stars have been shown to provide the natural testing grounds to explore the properties of strongly interacting matter, which is widely accepted to include neutron star (NS), quark star (QS), hybrid star (HS), and other compact objects with dense matter. Neutron stars are consistent with dense neutron-rich nuclear matter, which might be the remnants of massive stars after supernova explosions. NSs could be converted to the QSs whose possible existence is still one of the most important fields of modern nuclear physics and astrophysics [5–17]. In QSs, the isospin asymmetry caused by the unequal number of u and d quarks could be very large, which implies that the isovector interactions among SQM may be important in the strongly interacting matter, and the isospin asymmetric quark matter can also be formed in high-energy HICs at the BNL Relativistic Heavy Ion Collider (RHIC) and the Large Hadron Collider (LHC). Therefore, it is of great importance to explore the isospin effects in the isospin asymmetric quark matter, which is useful to study the properties of quark star physics, the hadron-quark phase transition in HSs, and the isospin dependence of the physical quantities in QCD phase diagram (the isovector properties of nuclear matter is still poorly known at finite baryon density and chemical potential). The recent works on the isovector properties of quark matter can be found in Refs. [18–31].

In 2013, the heavy pulsar PSR J0348+0432 with a mass of $2.01 \pm 0.04 M_\odot$ [32] was discovered, and in 2018 PSR J2215+5135 has been detected by fitting the radial velocity lines and the three-band light curves in the irradiated compact stars model with a much larger star mass as $2.27^{+0.17}_{-0.15} M_\odot$ [33]. In 2020, the newly discovered compact binary merger GW190814 [34] reported by the LIGO/Virgo Collaborations whose secondary component m_2 with a mass of $2.50 M_\odot - 2.67 M_\odot$ at 90% credible level has aroused lots of interest in the field of nuclear physics and astrophysics. From the observation results, the candidate of the secondary component of GW190814 can be considered as compact stars or light black hole, which sets very strict constraints on the EOS of strongly interacting matter once the candidate is considered as NSs or QSs. Moreover in 2019, the authors of Ref. [35] use the data of relativistic Shapiro delay with the Green Bank Telescope to report PSR J0740+6620 ($2.14 \pm^{0.10}_{0.09}$ $M_\odot$ with 68.3% credibility interval and $2.14 \pm^{0.20}_{0.18} M_\odot$ with 95.4% credibility interval) as the most massive precisely observed pulsar. In 2021, the star mass of PSR J0740+6620 has updated as $(2.08 \pm 0.07) M_\odot$ [36], and the radius of PSR J0740+6620 based on fits of rotating hot spot patterns to neutron star interior composition explorer (NICER) and x-ray multi-mirror (XMM-Newton) x-ray observations has been set as a more precise value as $13.7^{+2.6}_{-1.5}$ km (68%) [37]. Their results also show the full radius range spanning the $\pm 1\sigma$ credible intervals of all the radius estimates is 12.45 ± 0.65 km for a $1.4 M_\odot$ compact star and 12.35 ± 0.75 km for a $2.08 M_\odot$ compact star. In Ref. [38], the new measurement of the isolated 205.53 Hz millisecond pulsar PSR J0030+0451 with $R = 13.02^{+1.24}_{-1.06}$ km and $M = 1.44^{+0.15}_{-0.14} M_\odot$ is provided, and

*kyois@126.com
†lixiaohuaphysics@126.com
‡liuhe@qut.edu.cn
§jumin@upc.edu.cn
‖yingzhow@163.com

the circumferential radius and the gravitational mass of the compact star in 4U 1702-429 is estimated as $R = 12.4 \pm 0.4$ km and $M = 1.9 \pm 0.3 M_\odot$ from Ref. [39]. In the very recent work from Ref. [40], the authors estimate the radius and mass of the central compact object within the supernova remnant HESS J1731-347 to be $R = 10.4^{+0.86}_{-0.78}$ km and $M = 0.77^{+0.20}_{-0.17} M_\odot$ from Gaia observations. In the previous works, many quark phenomenological models used to produce massive quark star cases with strong isospin interaction inside the star matter [41–51]. On the other hand, the new observations and estimates of the mass-radius region for the supermassive compact stars we listed above indeed set very strict constraints on the EOS of SQM and may rule out most of the conventional phenomenological models of quark matter, and our main purpose of this work is to investigate the possible range of the parameter space for quark phenomenological models by considering the new mass-radius estimates, which may also set very strict constraints to the thermodynamical properties of the quark star matter and quark stars.

In the present work, we investigate the properties of the isospin chemical potential, the isospin asymmetry, the quark matter symmetry energy, the EOS of SQM, and the maximum mass of QSs under the new radius constraints of PSR J0740+6620 within quasiparticle model and isospin-density-dependent quark mass models. We find that the recent discovered supermassive compact stars can be well described as QSs within quasiparticle model under these new radius constraints.

II. THE THEORETICAL FORMULISM

A. The quasiparticle model

In recent works, phenomenological quark mass model has been widely used for exploring the thermodynamical properties of SQM and QSs [52–81], which mostly considers all the interactions among quarks into the equivalent quark mass or introduces effective bag constants. On the other side, with the results from the hard dense loop approximation [77], the quasiparticle model is proposed whose constituent quark mass expression can be written as [77,82,83]

$$m_q = \frac{m_{q_0}}{2} + \sqrt{\frac{m_{q_0}^2}{4} + \frac{g^2 \mu_q^2}{6\pi^2}}, \tag{1}$$

where m_{q0} means the quark current mass, and we set $m_{u0} = 5.5$ MeV, $m_{d0} = 5.5$ MeV, and $m_{s0} = 95$ MeV in this work. μ_q is the quark chemical potential, and g is the strongly interacting coupling constant which is considered as a free input parameter in this work.

The total thermodynamic potential density for SQM within quasiparticle model can be written as

$$\begin{aligned}\Omega &= \sum_i [\Omega_i + B_i(\mu_i)] + B \\ &= -\sum_i \frac{g_i}{48\pi^2}\left[\mu_i \sqrt{\mu_i^2 - m_i^2}\left(2\mu_i^2 - 5m_i^2\right)\right. \\ &\quad \left. + 3m_i^4 \ln \frac{\mu_i + \sqrt{\mu_i^2 - m_i^2}}{m_i}\right] + \sum_i B_i(\mu_i) + B, \end{aligned} \tag{2}$$

where B is the negative vacuum pressure term for nonperturbative confinement [84], and $B_i(\mu_i)$ is the additional chemical potential dependent terms and is expressed as

$$B_i(\mu_i) = -\int_{m_i}^{\mu_i} \frac{\partial \Omega_i}{\partial m_i} \frac{\partial m_i}{\partial \mu_i} d\mu_i. \tag{3}$$

The total energy density can be obtained as $\mathcal{E} = \sum_i \mathcal{E}_i$ with

$$\mathcal{E}_i = \frac{g_i}{2\pi^2} \int_0^\infty \left[\frac{\epsilon_i}{1 + e^{(\epsilon_i - \mu_i)/T}} + \frac{\epsilon_i}{1 + e^{(\epsilon_i + \mu_i)/T}}\right] p^2 dp, \tag{4}$$

where g_i means the degeneracy factor with $g_i = 6$ for quarks and $g_i = 2$ for leptons. The pressure P at zero temperature can be derived by considering

$$P = -\sum_i [\Omega_i + B_i(\mu_i)] - B. \tag{5}$$

B. The confined isospin- and density-dependent mass model

For comparison, we also employ the confined isospin- and density-dependent mass (CIDDM) model [24,79], whose equivalent mass is expressed as

$$\begin{aligned} m_q &= m_{q_0} + m_I + m_{\rm iso} \\ &= m_{q_0} + \frac{D}{{n_B}^z} - \tau_q \delta D_I n_B^\alpha e^{-\beta n_B}, \end{aligned} \tag{6}$$

where m_{q0} is bare quark mass, $m_I = \frac{D}{{n_B}^z}$ shows the flavor-independent quark interactions, and n_B means the baryon density of quark matter. In m_I term, the constant z is the equivalent mass scaling parameter and the constant D is determined by the absolutely stable condition of SQM. For the parameters in $m_{\rm iso}$ term, D_I is used to adjust the strength of the isospin interaction, α and β can determine the isospin-density dependence of the effective interactions in SQM, τ_q is the isospin quantum number of quarks, and the isospin asymmetry δ is defined as

$$\delta = 3\frac{n_d - n_u}{n_d + n_u}. \tag{7}$$

One can obtain the detailed calculation results of the EOS for SQM by considering the isospin and density-dependent quark mass within the CIDDM model from Ref. [79].

C. The isospin-dependent confining quark matter model

In Ref. [61], we insert the isospin-dependent mass term into the equivalent quark mass of the confining quark matter model, and the analytic expression is written as

$$M_i = m_i + m_i^* \mathrm{sech}\left(\nu_i \frac{n_B}{n_0}\right) - \tau_i \delta D_I n_B^\alpha e^{-\beta n_B}, \tag{8}$$

where n_0 is nuclear matter normal (saturation) density, and ν_i is a parameter determining the density dependence for quark mass. The readers can find the detailed discussions within IQCM model in Refs. [85–88].

D. Properties of quark matter at zero temperature

For SQM, people assume it is composed of u, d, and s quarks and leptons (e and μ) in beta-equilibrium. The weak

beta-equilibrium condition of SQM at zero temperature can be written as

$$\mu_d = \mu_s = \mu_u + \mu_e \quad \text{and } \mu_\mu = \mu_e. \tag{9}$$

Since the electric charge of SQM is neutral, the electric charge neutrality condition can be expressed as

$$\tfrac{2}{3}n_u = \tfrac{1}{3}n_d + \tfrac{1}{3}n_s + n_e + n_\mu. \tag{10}$$

In nuclear physics, symmetry energy is of great importance in understanding the isospin properties in quark star matter, and it can be obtained by expanding the energy per baryon in isospin asymmetry δ as

$$E(n_B, \delta, n_s) = E_0(n_B, n_s) + E_{\rm sym}(n_B, n_s)\delta^2 + O(\delta^4), \tag{11}$$

where $E_0(n_B, n_s) = E(n_B, \delta = 0, n_s)$ is the energy per baryon number in three-flavor u-d-s quark matter with an equal fraction of u and d quarks. Then the quark matter symmetry energy is expressed as

$$E_{\rm sym}(n_B, n_s) = \frac{1}{2}\frac{\partial^2 E(n_B, \delta, n_s)}{\partial \delta^2}\bigg|_{\delta=0}. \tag{12}$$

III. RESULTS AND DISCUSSIONS

A. Strange quark matter

From the conclusion of Farhi and Jaffe [9], SQM might be the true ground state and should satisfy the absolute stability, which means that the minimum value of the energy per baryon of SQM (udQM) (u-d quark matter) at zero temperature must be less (larger) than the minimum energy per baryon of the observed stable nuclei $M(^{56}\text{Fe})/56$ (930 MeV). To ensure the absolutely stable condition of SQM at zero temperature with quasiparticle model, we first choose the parameter sets as g-2.85 ($g = 2.85$, $B^{1/4} = 137$ MeV) and g-5.26 ($g = 5.26$, $B^{1/4} = 112$ MeV) in this section. Using these two parameter sets, one can describe the upper and lower radius limits of PSR J0740+6620 with $M = 2.08 \pm 0.07 M_\odot$ [36] by considering the constraint of the equatorial circumferential radius as $13.7^{+2.6}_{-1.5}$ km (68%) [37] in stable star matter (we define this constraint as Constraint A). Moreover, the results from Ref. [37] further tighten the allowed radius range at certain compact star masses by combining the NICER radius and mass measurements of PSR J0030+0451 and PSR J0740+6620, which provides the full radius range that spans the $\pm 1\sigma$ credible intervals of the radius estimate as 12.45 ± 0.65 km for a $1.4 M_\odot$ compact star and 12.35 ± 0.75 km for a $2.08 M_\odot$ compact star. Since the radius range is further narrowed down, we adjust the parameter space and set g-3.1 ($g = 3.1$, $B^{1/4} = 135$ MeV) and g-3.6 ($g = 3.6$, $B^{1/4} = 132$ MeV) to satisfy the lower and upper limits for the radius range by considering this new constraint (we define this constraint as Constraint B).

In Fig. 1, we calculate the energy per baryon and the corresponding pressure as functions of the baryon number density for SQM and two-flavor u-d quark matter (udQM) with g-2.85 and g-5.26 (here we consider Constraint A). One can find in Fig. 1 that the minimum energy per baryon of udQM is exactly 930 MeV while the minimum energy per baryon of SQM is smaller than 930 MeV, which satisfies the

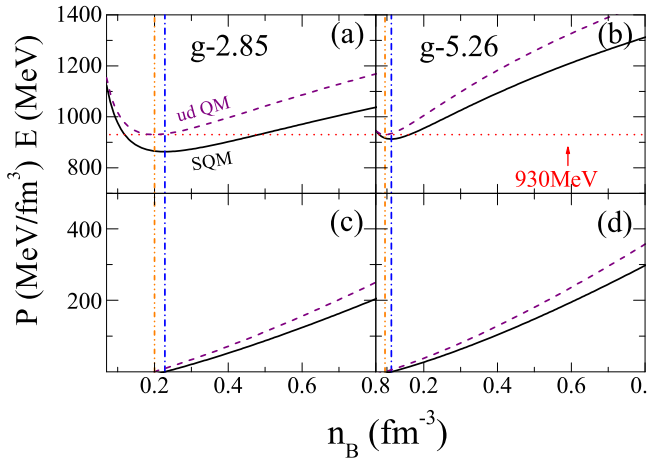

FIG. 1. The energy per baryon and pressure of SQM and udQM as functions of baryon number density with g-2.85 and g-5.26 within quasiparticle model.

absolutely stable condition. In the detailed calculation, we find the minimum energy per baryon of udQM decreases with the decrement of $B^{1/4}$ when the coupling constant g is fixed, and the EOS becomes stiffer with the decrement of $B^{1/4}$ with a fixed g, which indicates that the maximum star mass case cannot be obtained for the fixed g until the minimum energy per baryon of udQM decreases to 930 MeV (the lower limit by considering the absolutely stable condition for ud QM) with the decrement of $B^{1/4}$. Furthermore, it can also be seen from Fig. 1 that the baryon density of the minimum energy per baryon for SQM and udQM is exactly the corresponding baryon density of zero pressure point, which satisfies the requirement of thermodynamical self-consistency. Additionally, one can find the EOS of SQM gets stiffer with the coupling constant g. In Fig. 2, we calculate the EOS of SQM and udQM with g-3.1 and g-3.6 (here we consider Constraint B), and one can also find that the EOS for g-3.1 and g-3.6 satisfies the absolutely stable condition and the requirement of thermodynamical self-consistency. Moreover, one can find that

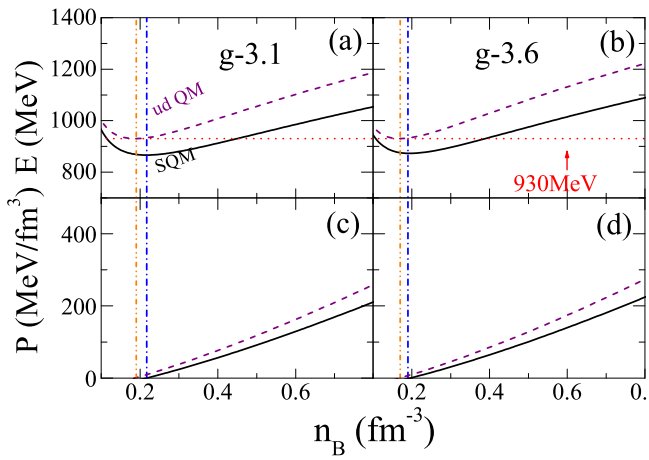

FIG. 2. The energy per baryon and pressure of SQM and udQM as functions of baryon number density with g-3.1 and g-3.6 within quasiparticle model.

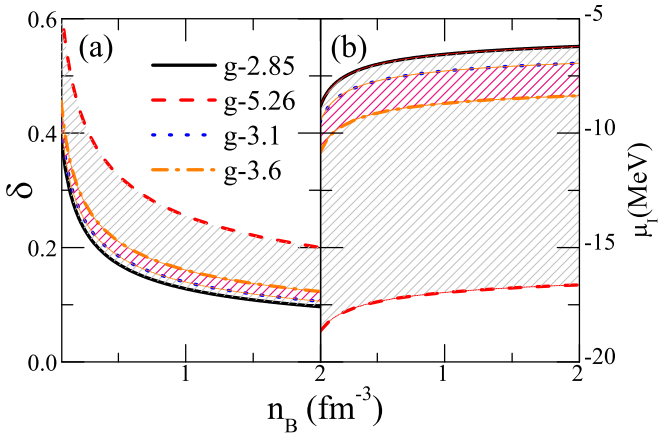

FIG. 3. δ and μ_I as functions of baryon density with different parameter sets within quasiparticle model.

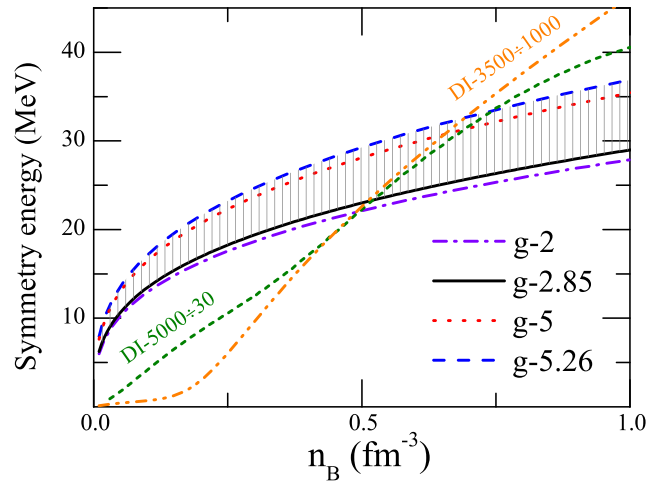

FIG. 4. Quark matter symmetry energy as functions of baryon density for Constraint A with different sets of parameters within quasiparticle model, CIDDM model, and ICQM model.

the pressure of SQM increases from 204 MeV to 297 MeV at $n_B = 0.8$ fm^{-3} with Constraint A, while the pressure for SQM with Constraint B increases from 211 to 224 MeV, which provides a significant reduction in the possible range of EOS for SQM to satisfy the radius constraints with Constraint B.

In Fig. 3, we calculate the isospin asymmetry and the isospin chemical potential [$\mu_I = (\mu_u - \mu_d)/2$] for SQM as functions of baryon density to discover the isospin properties of the star matter with g-2.85, g-5.26, g-3.1, and g-3.6 within quasiparticle model. It can be seen in Fig. 2 that the isospin chemical potential μ_I is negative and decreases (increases) with g (n_B), while the isospin asymmetry δ is positive and decreases with g and the baryon density, which implies that the quark star matter may become more isospin asymmetric with stiffer EOS at large g cases and one can find less isospin asymmetric quark matter in the central region of QSs. Moreover, we can find that the shaded area surrounded by the lines of g-3.1 and g-3.6 is much smaller than that of g-2.85 and g-5.26 case, which indicates that considering Constraint B can further reduce the parameter space of the isospin asymmetric quark star matter within quasiparticle model.

In Fig. 4, we calculate the quark matter symmetry energy as functions of baryon density with different parameter sets within quasiparticle model, CIDDM model, and ICQM model to investigate the isospin properties of quark matter. The parameter sets g-2.85 and g-5.26 are chosen to satisfy "Constraint A," and the parameter sets g-2 ($g = 2$, $B^{1/4} =$ 141 MeV) and g-5 ($g = 5$, $B^{1/4} = 120$ MeV) are used here mainly for comparison purposes (these two parameter sets are chosen to support the most massive QS cases by decreasing $B^{1/4}$ with a fixed g in the absolutely stable quark matter). From the results in Ref. [79], DI-3500 is the parameter set which is adjusted to support the maximum star mass ($M_{\rm star} = 2.39 M_\odot$) within CIDDM model ($z = 1.8$, $D_I = 3500$ MeV fm$^{3\alpha}$, $D =$ 13.81 MeV fm^{-3z}, $\alpha = 0.7$, and $\beta = 0.1$). For the parameter sets satisfying the absolutely stable condition within the ICQM model, the maximum quark star mass is calculated as $M_{\rm star} = 2.57 M_\odot$ by using DI-5000 ($D_I = 5000$ MeV fm$^{3\alpha}$ and $\nu_{ud} = 0.85$). One can find in Fig. 4 that the quark matter symmetry energy increases with baryon density in all the cases, and the values of the symmetry energy increases with the coupling constant g at a certain baryon density within quasiparticle model. The value of the symmetry energy at $n_B = 1$ fm^{-3} increases from 28.5 to 37 MeV when g increases from 2.85 to 5.26, and only the cases whose quark matter symmetry energy in the shaded region with the upper (lower) limit being g-2.85 (g-5.26) can satisfy Constraint A. It can also be seen in Fig. 4 that the quark matter symmetry energy predicted by DI-3500 from the CIDDM model or DI-5000 from the ICQM model is about 1000 times or 30 times the values of the symmetry energy for g-2 within quasiparticle model. In these two models, the quark mass is isospin and density dependent by introducing the isospin dependent term $\tau_i \delta D_I n_B^\alpha e^{-\beta n_B}$. From the results in Refs. [61,79], the quark matter symmetry energy increases rapidly with D_I, which can provide stiffer EOS of SQM to support massive QSs. On the other side, as D_I increases, the isospin asymmetry for quark star matter within the two models decreases with the quark matter symmetry energy, which further weaken the effects of D_I in the isospin-dependent mass term. Thus for large QSs (larger than two solar mass cases) within the CIDDM model and the ICQM model, the EOS of the star matter cannot be stiff enough to support the heavy stars with small values of D_I, and this is the reason why the quark matter symmetry energy with the CIDDM model and the ICQM model increases to a hundred times the symmetry energy of quasiparticle model to support massive QSs.

In Fig. 5, we calculate the symmetry energy as functions of baryon density with quasiparticle model, CIDDM model, and ICQM model. The parameter sets g-3.1 and g-3.6 are chosen to satisfy Constraint B. One can find that the shaded region is further narrowed down compared with Fig. 4, and the values of the upper and lower limits of the quark matter symmetry energy at $n_B = 1$ fm^{-3} for the shaded region from Constraint B are 31 and 29.5 MeV, which provides a much smaller range of the quark matter symmetry energy to satisfy Constraint B within quasiparticle model.

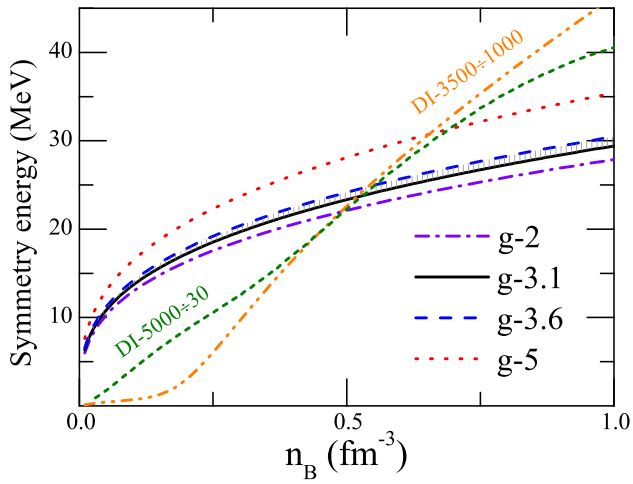

FIG. 5. Quark matter symmetry energy as functions of baryon density for Constraint B with different parameter sets within quasiparticle model, CIDDM model, and ICQM model.

In Fig. 6, we examine the sound velocity with different parameter sets discussed before within quasiparticle model, and one can see that the sound velocity from the listed cases exhibits less than the speed of light, which satisfies the causality condition $c_s < c$. One can also find in Fig. 6 that the sound velocity decreases with g. From the results of the quark matter within quasiparticle model from Fig. 1 to Fig. 5, we can obtain the conclusion that large quark matter symmetry energy can decrease the sound speed of quark matter and stiffen the EOS of SQM within quasiparticle model, which might support more massive QSs.

B. Quark stars

In Fig. 7, we calculate the mass-radius lines for different sets of parameters within CIDDM model (DI-3500),

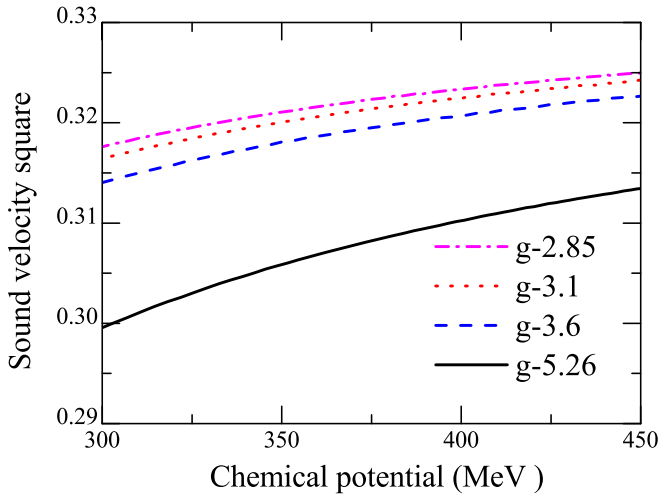

FIG. 6. Sound velocity square as functions of the chemical potential $\mu_B = \frac{1}{3}(\mu_u + \mu_d + \mu_s)$ with different sets of parameters within quasiparticle model at zero temperature.

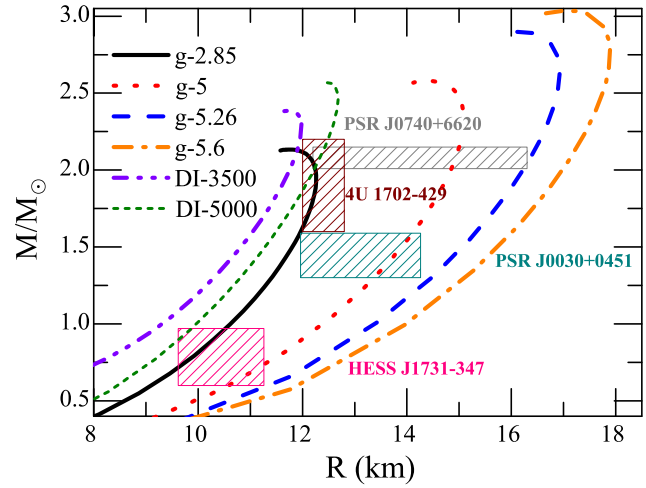

FIG. 7. Mass-radius relation for different sets of parameters within CIDDM model and quasiparticle model. The gray shaded region with $R = 13.7^{+2.6}_{-1.5}$ km and $M = 2.08 \pm 0.07 M_\odot$ is the newly updated constraint of PSR J0740+6620 calculated in Ref. [37] (Constant A).

ICQM model (DI-5000), and quasiparticle model [g-2.85, g-5, g-5.26, and g-5.6 ($g = 5.6$, $B^{1/4} = 108.9$ MeV)]. The gray shaded region with $R = 13.7^{+2.6}_{-1.5}$ km and $M = 2.08 \pm 0.07 M_\odot$ is the newly updated constraint of PSR J0740+6620 calculated in Ref. [37] (Constraint A), the pink shaded region with $R = 10.4^{+0.86}_{-0.78}$ km and $M = 0.77^{+0.20}_{-0.17} M_\odot$ is the estimate from the central compact object within the supernova remnant HESS J1731-347 [40] (Constraint C), the dark cyan shaded region with $R = 13.02^{+1.24}_{-1.06}$ km and $M = 1.44^{+0.15}_{-0.14} M_\odot$ is the measurement for the isolated 205.53 Hz millisecond pulsar PSR J0030+0451 [38] (Constraint D), and the wine shaded region with $R = 12.4 \pm 0.4$ km and $M = 1.9 \pm 0.3 M_\odot$ is the estimate for 4U 1702-429 [39] (Constraint E). One can obtain from Fig. 7 that the maximum mass and the radius of QSs both increase with the coupling constant g within quasiparticle model. Furthermore, we can see that the mass-radius line of g-2.85 with the maximum star mass of $2.13 M_\odot$ can reach the left boundary of Constraint A, while the mass-radius line of g-5.26 with the maximum star mass of 2.90 solar mass can reach the right boundary of Constraint A. From the discussion in Fig. 1, $2.13 M_\odot$ and $2.90 M_\odot$ are the maximum star-mass cases $g = 2.85$ and $g = 5.26$ can support, respectively. This result shows the lower and upper limits for the chosen region of the coupling constant g by considering Constraint A, and this is also the reason why we choose g-3.1 and g-3.6 for Constraint B. From the results in Figs. 1, 3, 4, and 7, one can also find that considering Constraint A indeed put strict constraints on the EOS of SQM, the quark matter symmetry energy, and the mass-radius relation lines within quasiparticle model, which further reduces the corresponding parameter space. Moreover, for DI-3500 case (which is capable of supporting the maximum star mass $M = 2.39 M\odot$ for the CIDDM model) and g-5.6 case (which is capable of supporting the maximum star mass $M = 3.03 M\odot$ for quasiparticle model), the mass-radius lines cannot satisfy Constraint A (the DI-3500 case can only reach the left boundary of the wine area for Constraint

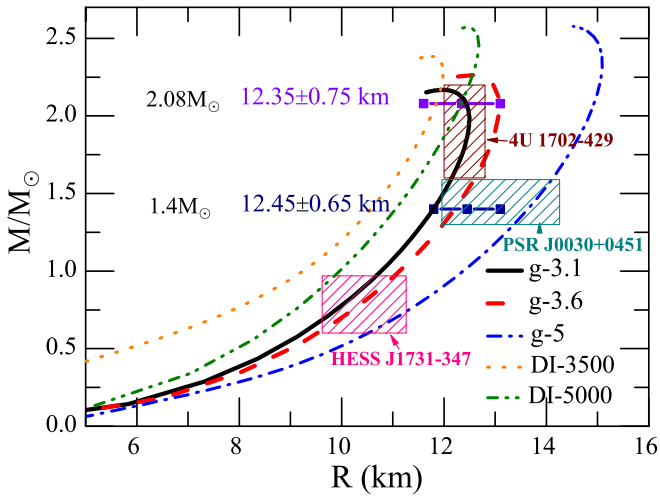

FIG. 8. The maximum mass of QSs as functions of radius with different parameter sets within quasiparticle model. The constraints of the radius at 2.08 and 1.4 solar mass are provided by considering different frameworks of EOSs modeling in Ref. [37] (Constraint B).

E), while for the DI-5000 case (which is capable of supporting the maximum star mass $M = 2.57M\odot$ for the ICQM model), the mass-radius lines is able to satisfy Constraints A and E. For g-5 case, which can describe the GW190814's secondary component as QSs ($2.59M_\odot$) within quasiparticle model, the mass-radius line can satisfy Constraints A, C, and D, while for g-2.85 case all the constraints listed are satisfied.

In Ref. [37], the authors also show the full radius range that spans the $\pm 1\sigma$ credible intervals of the radius estimate in several frameworks as 12.45 ± 0.65 km for a $1.4M_\odot$ compact star and 12.35 ± 0.75 km for a $2.08M_\odot$ compact star, which further narrows down the radius range at a certain star mass and sets a new challenge for phenomenological quark models to search for the parameter space satisfying the radius constraints (Constraint B). Then we calculate the mass-radius for different sets of parameters within the CIDDM model (DI-3500), the ICQM model (DI-5000), and the quasiparticle model (g-3.1, g-3.6, and g-5) by considering Constraints B–E. From the results of Fig. 8, one can find the mass-radius line for g-3.1 reaches exactly the left limit of 12.45 ± 0.65 km for $M = 1.4M_\odot$ from Constraint B, while the mass-radius line for g-3.6 reaches the right limit of 12.35 ± 0.75 km for $M = 2.08M_\odot$ from Constraint B. One can also find that the mass-radius lines of the DI-3500, DI-5000, and g-5 cases cannot satisfy the two ranges of Constraint B, which indicates that considering Constraint B indeed sets much stricter constraints on the parameter chosen space compared with Constraint A. Our results indicate that only the mass-radius lines appears in the range between g-3.1 and g-3.6 within quasiparticle model can satisfy all the constraints (Constraints B–E) we listed (the mass-radius lines for CIDDM model and ICQM model cannot describe QSs by considering these constraints, which means the density-dependent quark mass models need further modifying), and the parameter space of the corresponding EOS within quasiparticle model is further constrained by considering these mass-radius estimates.

IV. CONCLUSION AND DISCUSSION

In this work, we explore the properties of isospin asymmetric quark matter in quark stars. The isospin chemical potential, the isospin asymmetry, the quark matter symmetry energy, the EOS of SQM, and the maximum mass of QSs are also studied by using the quark quasiparticle model, the CIDDM model, and the ICQM model.

We first calculate the isospin chemical and isospin asymmetry to discover the properties of the isospin asymmetric quark matter, and the quark matter symmetry energy is also discussed in this work. Our result indicates that large quark matter symmetry energy can stiffen the EOS of the star matter. Moreover, we also calculate the maximum mass of the quark stars by considering different mass-radius measurement constraints, and we find the mass-radius measurements can reduce the parameter chosen range of the quark matter symmetry energy and the EOS of SQM. Especially when the new estimates of PSR J0740+6620, HESS J1731-347, and PSR J0030+0451 are considered, the range of the mass-radius line within quasiparticle model is further limited, while the mass-radius lines within the CIDDM model and the ICQM model cannot satisfy all the constraints of these new measurements and estimates.

Therefore, our results have demonstrated that the new radius measurements indeed put very strict constraints on the possible range of the parameter space of the EOS of SQM, the quark matter symmetry energy (the isospin effects), as well as the maximum mass of QSs within the quasiparticle model.

In the present work, we mainly focus on investigating the properties of quark star matter and QSs by fitting the recent measurements of compact star mass and radius within the CIDDM model, the ICQM model, and the quasiparticle model. Although the mass-radius lines provided by quasiparticle model may be better at satisfying most of the recent star mass and radius estimates in this work than the other two models, we should mention that the EOS of quark matter calculated within quasiparticle model may still not be the correct representation of the true EOS of quark star matter (for example, the bag constant treatment in quasiparticle model should be modified in future works). Furthermore, the CIDDM model and the ICQM model can also be used to describe the recent compact star estimates by modifying the equivalent quark mass forms or consider introducing isovector-interaction terms inside the phenomenological models, which may also stiffen the EOS of quark star matter. Moreover, we can consider color-flavor-locked (CFL) quark matter around the core region of the compact star, where the EOS of the star matter may be increased by the energy gap Δ, and these works are in progress.

ACKNOWLEDGMENTS

This work is supported by the National Natural Science Foundation of China under Grants No. 11975132, No. 12205158, and No. 11505100, and the Shandong Provincial Natural Science Foundation, China under Grants No. ZR2022JQ04, No. ZR2021QA037, No. ZR2019YQ01 and No. ZR2015AQ007.

[1] N. K. Glendenning, *Compact Stars*, 2nd ed. (Spinger-Verlag New York, 2000).
[2] F. Weber, *Pulsars as Astrophysical Laboratories for Nuclear and Particle Physics* (IOP Publishing, Ltd, London, 1999).
[3] J. M. Lattimer and M. Prakash, Science **304**, 536 (2004).
[4] A. W. Steiner, M. Prakash, J. M. Lattimer, and P. J. Ellis, Phys. Rep. **411**, 325 (2005).
[5] D. Ivanenko and D. F. Kurdgelaidze, Lettere al Nuovo Cimento, **2**, 13 (1969).
[6] N. Itoh, Prog. Theor. Phys. **44**, 291 (1970).
[7] A. R. Bodmer, Phys. Rev. D **4**, 1601 (1971).
[8] E. Witten, Phys. Rev. D **30**, 272 (1984).
[9] E. Farhi and R. L. Jaffe, Phys. Rev. D **30**, 2379 (1984).
[10] C. Alcock, E. Farhi, and A. Olinto, Astrophys. J. **310**, 261 (1986).
[11] F. Weber, Prog. Part. Nucl. Phys. **54**, 193 (2005).
[12] I. Bombaci, I. Parenti, and I. Vidana, Astrophys. J. **614**, 314 (2004).
[13] J. Staff, R. Ouyed, and M. Bagchi, Astrophys. J. **667**, 340 (2007).
[14] M. Herzog and F. K. Röpke, Phys. Rev. D **84**, 083002 (2011).
[15] H. Terazawa, INS-Report-338 (INS, Univ. of Tokyo, 1979).
[16] M. A. Stephanov, K. Rajagopal, and E. V. Shuryak, Phys. Rev. Lett. **81**, 4816 (1998).
[17] P. C. Chu *et al.*, Eur. Phys. J. C **81**, 569 (2021).
[18] D. T. Son and M. A. Stephanov, Phys. Rev. Lett. **86**, 592 (2001).
[19] M. Frank, M. Buballa, and M. Oertel, Phys. Lett. B **562**, 221 (2003).
[20] D. Toublan and J. B. Kogut, Phys. Lett. B **564**, 212 (2003).
[21] J. B. Kogut and D. K. Sinclair, Phys. Rev. D **70**, 094501 (2004).
[22] L. He, M. Jin, and P. Zhuang, Phys. Rev. D **71**, 116001 (2005).
[23] L. He and P. Zhuang, Phys. Lett. B **615**, 93 (2005).
[24] P. C. Chu, L. W. Chen, and X. Wang, Phys. Rev. D **90**, 063013 (2014).
[25] P. C. Chu, Y. Zhou, X. Qi, X. H. Li, Z. Zhang, and Y. Zhou, Phys. Rev. C **99**, 035802 (2019).
[26] P. C. Chu, Y. Zhou, X. H. Li, and Z. Zhang, Phys. Rev. D **100**, 103012 (2019).
[27] P. C. Chu *et al.*, Eur. Phys. J. C **81**, 93 (2021).
[28] M. Di Toro, A. Drago, T. Gaitanos, V. Greco, and A. Lavagno, Nucl. Phys. A **775**, 102 (2006).
[29] Z. Zhang and Y. X. Liu, Phys. Rev. C **75**, 064910 (2007).
[30] G. Pagliara and J. Schaffner-Bielich, Phys. Rev. D **81**, 094024 (2010).
[31] G. Y. Shao, M. Colonna, M. Di Toro, B. Liu, and F. Matera, Phys. Rev. D **85**, 114017 (2012).
[32] J. Antoniadis *et al.*, Science **340**, 1233232 (2013).
[33] M. Linares, T. Shahbaz, and J. Casares, Astrophys. J. Lett. **859**, 54 (2018).
[34] R. Abbott *et al.*, Astrophys. J. Lett. **896**, L44 (2020).
[35] H. Thankful Cromartie *et al.*, Nat. Astron. **4**, 72 (2020).
[36] E. Fonseca *et al.*, Astrophys. J. Lett. **915**, L12 (2021).
[37] M. C. Miller *et al.*, Astrophys. J. Lett. **918**, L28 (2021).
[38] M. C. Miller *et al.*, Astrophys. J. Lett. **887**, L24 (2019).
[39] J. Nättilä *et al.*, Astron. Astrophys. **608**, A31 (2017).
[40] V. Doroshenko, V. Suleimanov, G. Phlhofer, and A. Santangelo, Nat. Astron. **6**, 1444 (2022).
[41] M. Alford and S. Reddy, Phys. Rev. D **67**, 074024 (2003).
[42] M. Alford, P. Jotwani, C. Kouvaris, J. Kundu, and K. Rajagopal, Phys. Rev. D **71**, 114011 (2005).
[43] M. Baldo, Phys. Lett. B **562**, 153 (2003).
[44] N. D. Ippolito, M. Ruggieri, D. H. Rischke, A. Sedrakian, and F. Weber, Phys. Rev. D **77**, 023004 (2008).
[45] X. Y. Lai and R. X. Xu, Res. Astron. Astrophys. **11**, 687 (2011).
[46] M. G. B. de Avellar, J. E. Horvath, and L. Paulucci, Phys. Rev. D **84**, 043004 (2011).
[47] L. Bonanno and A. Sedrakian, Astron. Astrophys. **539**, A16 (2012).
[48] P. C. Chu, B. Wang, Y. Y. Jia, Y. M. Dong, S. M. Wang, X. H. Li, L. Zhang, X. M. Zhang, and H. Y. Ma, Phys. Rev. D **94**, 123014 (2016).
[49] P. C. Chu *et al.*, Eur. Phys. J. C **77**, 512 (2017).
[50] P. C. Chu *et al.*, J. Phys. G **47**, 085201 (2020).
[51] Z. Zhang, P. C. Chu, X. H. Li, H. Liu, and X. M. Zhang, Phys. Rev. D **103**, 103021 (2021).
[52] A. Chodos, R. L. Jaffe, K. Ohnson, C. B. Thorn, and V. F. Weisskopf, Phys. Rev. D **9**, 3471 (1974).
[53] M. Alford, M. Braby, M. Paris, and S. Reddy, Astrophys. J. **629**, 969 (2005).
[54] P. Rehberg, S. P. Klevansky, and J. Hüfner, Phys. Rev. C **53**, 410 (1996).
[55] M. Hanauske, L. M. Satarov, I. N. Mishustin, H. Stocker, and W. Greiner, Phys. Rev. D **64**, 043005 (2001).
[56] S. B. Rüster and D. H. Rischke, Phys. Rev. D **69**, 045011 (2004).
[57] D. P. Menezes, C. Providência, and D. B. Melrose, J. Phys. G **32**, 1081 (2006).
[58] J. Chao, P. Chu, and M. Huang, Phys. Rev. D **88**, 054009 (2013).
[59] P. C. Chu, X. Wang, L. W. Chen, and M. Huang, Phys. Rev. D **91**, 023003 (2015).
[60] P. C. Chu, B. Wang, H. Y. Ma, Y. M. Dong, S. L. Chang, C. H. Zheng, J. T. Liu, and X. M. Zhang, Phys. Rev. D **93**, 094032 (2016).
[61] P. C. Chu and L. W. Chen, Phys. Rev. D **96**, 083019 (2017).
[62] C. D. Roberts and A. G. Williams, Prog. Part. Nucl. Phys. **33**, 477 (1994), and references therein.
[63] H. S. Zong, L. Chang, F. Y. Hou, W. M. Sun, and Y. X. Liu, Phys. Rev. C **71**, 015205 (2005).
[64] S. X. Qin, L. Chang, H. Chen, Y. X. Liu, and C. D. Roberts, Phys. Rev. Lett. **106**, 172301 (2011).
[65] B. A. Freedman and L. D. Mclerran, Phys. Rev. D **16**, 1169 (1977).
[66] E. S. Fraga, R. D. Pisarski, and J. Schaffner-Bielich, Phys. Rev. D **63**, 121702 (2001).
[67] E. S. Fraga and P. Romatschke, Phys. Rev. D **71**, 105014 (2005).
[68] A. Kurkela, P. Romatschke, and A. Vuorinen, Phys. Rev. D **81**, 105021 (2010).
[69] G. N. Fowler, S. Raha, and R. M. Weiner, Z. Phys. C: Part. Fields **9**, 271 (1981).
[70] S. Chakrabarty, S. Raha, and B. Sinha, Phys. Lett. B **229**, 112 (1989).
[71] S. Chakrabarty, Phys. Rev. D **43**, 627 (1991); **48**, 1409 (1993); **54**, 1306 (1996).
[72] O. G. Benvenuto and G. Lugones, Phys. Rev. D **51**, 1989 (1995).
[73] G. X. Peng, H. C. Chiang, J. J. Yang, L. Li, and B. Liu, Phys. Rev. C **61**, 015201 (1999).

[74] G. X. Peng, H. C. Chiang, B. S. Zou, P. Z. Ning, and S. J. Luo, Phys. Rev. C **62**, 025801 (2000).
[75] G. X. Peng, A. Li, and U. Lombardo, Phys. Rev. C **77**, 065807 (2008).
[76] A. Li, G. X. Peng, and J. F. Lu, Res. Astron. Astrophys. **11**, 482 (2011).
[77] K. Schertler, C. Greiner, and M. H. Thoma, Nucl. Phys. A **616**, 659 (1997).
[78] K. Schertler, C. Greiner, P. K. Sahu, and M. H. Thoma, Nucl. Phys. A **637**, 451 (1998).
[79] P. C. Chu and L. W. Chen, Astrophys. J. **780**, 135 (2014).
[80] P. C. Chu *et al.*, Phys. Lett. B **778**, 447 (2018).
[81] P. C. Chu and L. W. Chen, Phys. Rev. D **96**, 103001 (2017).
[82] R. D. Pisarski, Nucl. Phys. A **498**, 423 (1989).
[83] X. J. Wen *et al.*, J. Phys. G **36**, 025011 (2009).
[84] B. K. Patra and C. P. Singh, Phys. Rev. D **54**, 3551 (1996).
[85] M. Dey, I. Bombaci, J. Dey, S. Ray, and B. C. Samanta, Phys. Lett. B **438**, 123 (1998).
[86] J. L. Richardson, Phys. Lett. B **82**, 272 (1979).
[87] J. I. Kapusta, Phys. Rev. D **20**, 989 (1979).
[88] M. Bagchi, S. Ray, M. Dey, and J. Dey, Astron. Astrophys. **450**, 431 (2006).